

Effect of scalar leptoquarks on the lepton flavor violation decays of B meson

Jin-Huan Sheng^{1,2,3*}, Ru-Min Wang^{3,†}, Ya-Dong Yang^{1,2‡}

¹ *Central China Normal University, Wuhan, Hubei 430079, P.R.China*

² *Institute of Particle Physics and Key Laboratory of Quark and Lepton Physics (MOE)*

³ *College of Physics and Electronic Engineering, Xinyang Normal University, Xinyang, Henan 464000, P.R.China*

Abstract

Leptoquarks have been suggested to solve a variety of discrepancies between the expected and observed phenomenon. In this paper, we investigate the effect of scalar leptoquarks on the lepton flavor violating B meson rare decays which involve the quark level transition $\bar{b} \rightarrow \bar{s}\ell_i^-\ell_j^+ (i \neq j)$. The leptoquark parameter space is constrained by using the recently measured upper limits on the $\mathcal{B}(B_s^0 \rightarrow \ell_i^-\ell_j^+)$ and $\mathcal{B}(B \rightarrow K^{(*)}\ell_i^-\ell_j^+)$. Using such constrained leptoquark parameter space, some relevant physical quantities are also predicted and we find that the constrained New Physics parameters in the leptoquark model have very obvious effects on the relevant physical quantities in this paper. With future measurements of observable in $B \rightarrow K^{(*)}\ell_i^-\ell_j^+$ decays at the LHCb, more and more differentiated from the other NP explanations could be tested.

Key words: Leptoquark; Lepton flavor violating; Lepton number violating

PACS Numbers: 13.20.He, 12.15.Mm, 14.80.Sv

*jinhuanwuli@126.com

†ruminwang@sina.com

‡yangyd@mail.ccnu.edu.cn

1 Introduction

In recent times, the study for rare decays of B meson induced by the flavor changing neutral current (FCNC) process $b \rightarrow s(d)$ play a very important role to test the standard model (SM) and to provide crucial information in our search for New Physics(NP) beyond SM. The SM contributions to the rare B meson decays which involve FCNC process $b \rightarrow s(d)$ are absent at the tree level due to the Glashow-Iliopoulos-Maiani(GIM) mechanism and occur via the one-loop level. At the same time we find the result of $\mathcal{B}(B \rightarrow K^{(*)}\mu^-\mu^+)/\mathcal{B}(B \rightarrow K^{(*)}e^-e^+)$ in LHCb measurements deviate from the SM predictions (≈ 1) by $2-3\sigma$ [1] and the other notable deviations angular observable P'_5 between theory [2] and experiments [3, 4] for $B \rightarrow K^*\mu^-\mu^+$.

The lepton flavor violating (LFV) decay of the process $\ell \rightarrow \ell\gamma$, $Z \rightarrow \ell\bar{\ell}'$ and $h \rightarrow \mu\tau$ have been searched in LEP1, International Linear Collider(ILC) and CMS [5–7]. The lepton flavor non-universality of process $\bar{b} \rightarrow \bar{s}\ell^-\ell^+$ decays imply LFV processes may be seen in B decays [8, 9]. The experimental observation for the LFV decays will provide unambiguous signal for NP beyond the SM. In this paper, we will investigate the LFV of B meson decay process $\bar{b} \rightarrow \bar{s}\ell_i^-\ell_j^+ (i \neq j)$ in the scalar leptoquark model.

It is well known that leptoquarks (LQs) are color-triplet bosonic particle which can couple to a quark and a lepton at the same time and can occur in various extensions of the SM [10, 11]. They can also have spin-1 (vector leptoquarks) or spin-0 (scalar leptoquarks). In this article, we are intended to investigate the effect of scalar leptoquarks on the LFV $B_s \rightarrow \ell_i^-\ell_j^+$ and $B \rightarrow K^{(*)}\ell_i^-\ell_j^+$ processes. Scalar leptoquarks can exist at TeV scale in extended technicolor models [12, 13] as well as in quark and lepton composite models [14]. The phenomenology of scalar leptoquarks have been studied extensively in many literature [15–23]. It is generally assumed that the vector leptoquarks tend to couple directly to neutrinos, and hence it is expected that their couplings are tightly constrained from the neutrino mass and mixing data. Therefore, in this paper we only consider the model where leptoquarks can couple to a pair of quarks and leptons and may be inert with respect to proton decay. Hence, the bounds from proton decay may not be applicable for such cases and leptoquarks may produce signatures in other low-energy phenomena [23].

In this paper the upper limits on the relevant lepton number violating (LNV) coupling products due to the exchanges of scalar leptoquarks are obtained from the recent limits of

$\mathcal{B}(B_s \rightarrow \ell_i^- \ell_j^+)$ and $\mathcal{B}(B \rightarrow K^{(*)} \ell_i^- \ell_j^+)$ and shown in detailed in this paper. We also examine the constrained effects on these decays and we find there are very obvious NP coupling effects on the dileptonic invariant mass spectra, the single lepton longitudinal polarization asymmetries and the forward-backward asymmetries.

The outline of this paper is follows: In section 2, we recapitulate briefly New physics contribution to the LFV decays $b \rightarrow s \ell_i^- \ell_j^+$ in the scalar leptoquark model. In section 3 we present the numerical analysis for the branching ratios and other physical observed quantity. Section 4 contains the summary and conclusion.

2 New physics contribution to the LFV decays $b \rightarrow s \ell_i^- \ell_j^+$ due to scalar leptoquarks

As is known to all, the family lepton number (L_e, L_μ, L_τ) are exactly conserved in the standard model. Consequently, the lepton flavor violation processes are absolutely forbidden in the SM. In this paper we mainly investigate LFV process $\bar{b} \rightarrow \bar{s} \ell_i^- \ell_j^+$ in scalar leptoquark model due to the exchange of leptoquarks.

As discussed in other articles [23–31], out of all possible leptoquark multiplets we will consider the minimal renormalizable scalar leptoquark models, containing one single additional representation of $SU(3) \times SU(2) \times U(1)$ and which do not allow proton decay at the tree level. The scalar leptoquark multiplets can have the representation as $X = (3, 2, 7/6)$ and $X = (3, 2, 1/6)$ under the gauge group $SU(3) \times SU(2) \times U(1)$. Our objective in this paper is consider these scalar leptoquarks, which contribute to the process $\bar{b} \rightarrow \bar{s} \ell \ell$ and constrain the couplings from the experimental data of $B_s \rightarrow \ell_i^- \ell_j^+$ and $B \rightarrow K^{(*)} \ell_i^- \ell_j^+$

These scalar leptoquarks can have sizable Yukawa couplings and could potentially contribute to the quark level transition $b \rightarrow q \ell^- \ell^+$. The tree level Feynman diagram for the LFV process $b \rightarrow s \ell^- \ell^+$ are depicted in Fig.1. Owing to the chirality, diagonality nature and the conservation of both baryon and lepton number, these leptoquarks processes will provide an effective way looking for their effects in rare B meson decays. The details of new contributions have been explicitly discussed in Refs. [23–28] and here we outline the main points simply. There are two Lagrangian for process $\bar{b} \rightarrow \bar{s} \ell \ell$ due to the coupling of scalar leptoquark $X=(3,2,7/6)$ and

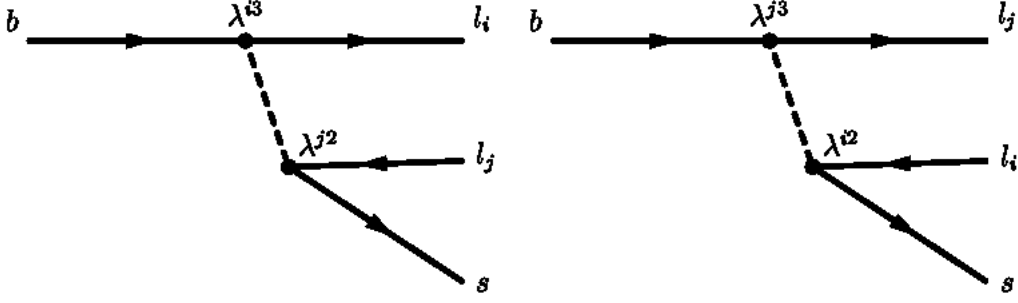


Figure 1: Feynman diagram for the process $b \rightarrow sl_i^- l_j^+$ (left) and $b \rightarrow sl_i^+ l_j^-$ (right) due to the scalar leptoquark exchange where $l = e, \mu, \tau$.

$X=(3,2,1/6)$ and fermion bilinear respectively.

Mold A: $X=(3, 2, 7/6)$

In this mold the interaction Lagrangian is given as

$$\mathcal{L} = -\lambda_u^{ij} \bar{u}_R^i X^T \epsilon L_L^j - \lambda_e^{ij} \bar{e}_R^i X^\dagger Q_L^j + h.c. \quad (1)$$

where i, j are the generation indices, Q_L and L_L are the left handed quark and lepton doublets, u_R and e_R are the right handed up-type quark and charged lepton singlets and $\epsilon = i\sigma_2$ is a 2×2 matrix. More explicitly these multiplets can be found in Refs. [23–28]. The use of Fierz transformation, leads to the leptoquark effective Hamiltonian for the process $\bar{b} \rightarrow \bar{s} \ell_i^- \ell_j^+$ as

$$\mathcal{H}_{LQ} = \frac{\lambda^{i3} \lambda^{j2*}}{8M_Y^2} [\bar{s} \gamma^\mu (1 - \gamma_5) b] [\bar{\ell}_i \gamma_\mu (1 + \gamma_5) \ell_j] = G_{LQ}^{\frac{7}{6}} [\bar{s} \gamma^\mu (1 - \gamma_5) b] [\bar{\ell}_i \gamma_\mu (1 + \gamma_5) \ell_j]. \quad (2)$$

Mold B: $X=(3, 2, 1/6)$

In this mold the interaction Lagrangian is given as

$$\mathcal{L} = -\lambda_d^{ij} \bar{d}_{\alpha R}^i (V_\alpha e_L^j - Y_\alpha \nu_L^j) + h.c. , \quad (3)$$

where the notations used are the same as the previous case. The leptoquark effective Hamiltonian are gotten with the same approach above

$$\mathcal{H}_{LQ} = \frac{\lambda^{2i} \lambda^{3j*}}{8M_Y^2} [\bar{s} \gamma^\mu (1 + \gamma_5) b] [\bar{\ell}_i \gamma_\mu (1 - \gamma_5) \ell_j] = G_{LQ}^{\frac{1}{6}} [\bar{s} \gamma^\mu (1 + \gamma_5) b] [\bar{\ell}_i \gamma_\mu (1 - \gamma_5) \ell_j]. \quad (4)$$

After theoretically analyzing and comparing, we find the current matrix elements of hamiltonian in mold B are same with the structure of R-Parity Violation for process $b \rightarrow s\ell_i^-\ell_j^+$ in our previous work [32]. This will lead to that variation trend of many physical observed quantity are very similar with the result of our previous paper. Further more, from Eq. (2) and Eq. (4) one can see difference of the current matrix elements is that replace $1 \pm \gamma_5$ with $1 \mp \gamma_5$. However, the effect on these differences is not significant except the single lepton longitudinal polarization asymmetries in the final result of two molds.

2.1 The $B_s \rightarrow \ell_i^-\ell_j^+$ decays

Using the above information, we can get total decay branching ratios

$$\mathcal{B}(B_s \rightarrow \ell_i^-\ell_j^+) = \frac{\tau_{B_s}\sqrt{\lambda(m_{B_s}^2, m_{\ell_i}^2, m_{\ell_j}^2)}}{4\pi m_{B_s}^3} \left\{ |G_{LQ}f_{B_s}|^2 \left[m_{B_s}^2(m_{\ell_i}^2 + m_{\ell_j}^2) - (m_{\ell_i}^2 - m_{\ell_j}^2)^2 \right] \right\} 5$$

with G_{LQ} is $G_{LQ}^{\frac{1}{6}}(G_{LQ}^{\frac{7}{6}})$ and $\lambda(a, b, c) \equiv a^2 + b^2 + c^2 - 2ab - 2ac - 2bc$ and this result is consistent with the expression in Ref. [24].

2.2 The $B \rightarrow K^{(*)}\ell_i^-\ell_j^+$ decays

Similar with the squark section of Eqs. (6) and (7) in our previous paper about R-Parity violating [32]. we can also get the differential decay distribution for these semileptonic decays with respects to s

$$\begin{aligned} \frac{d\Gamma(B \rightarrow K\ell_i^-\ell_j^+)}{ds} &= \frac{u(s)|G_{LQ}|^2}{2^8\pi^3 m_{B_s}^3} \left\{ \left[|H_t(q^2)|^2 \left(\left| h_{\frac{1}{2}, \frac{1}{2}} \right|^2 + \left| h_{-\frac{1}{2}, -\frac{1}{2}} \right|^2 \right) \right. \right. \\ &\quad \left. \left. + \frac{1}{3} |H_0(q^2)|^2 \left(\left| h_{\frac{1}{2}, \frac{1}{2}} \right|^2 + \left| h_{-\frac{1}{2}, \frac{1}{2}} \right|^2 + \left| h_{\frac{1}{2}, -\frac{1}{2}} \right|^2 + \left| h_{-\frac{1}{2}, -\frac{1}{2}} \right|^2 \right) \right] \right\}, \end{aligned} \quad (6)$$

$$\begin{aligned} \frac{d\Gamma(B \rightarrow K^*\ell_i^-\ell_j^+)}{ds} &= \frac{u(s)|G_{LQ}|^2}{2^8\pi^3 m_{B_s}^3} \left\{ \left[|H_{0t}|^2 \left(\left| h_{\frac{1}{2}, \frac{1}{2}} \right|^2 + \left| h_{-\frac{1}{2}, -\frac{1}{2}} \right|^2 \right) + \frac{1}{3} \left(|H_{00}|^2 + |H_{++}|^2 + |H_{--}|^2 \right) \right. \right. \\ &\quad \left. \left. \times \left(\left| h_{\frac{1}{2}, \frac{1}{2}} \right|^2 + \left| h_{-\frac{1}{2}, \frac{1}{2}} \right|^2 + \left| h_{\frac{1}{2}, -\frac{1}{2}} \right|^2 + \left| h_{-\frac{1}{2}, -\frac{1}{2}} \right|^2 \right) \right] \right\}, \end{aligned} \quad (7)$$

In addition, there are other physical observed quantity which are not discussed in many references are also investigated in this paper due to scalar leptoquark exchange. The definition formula of forward-backward asymmetries are got from Refs. [32, 33]. We get the specific expressions of $\mathcal{A}_{FB}(B \rightarrow$

$K^{(*)}\ell_i^-\ell_j^+(s)$ in the scalar leptoquark model. There are differences between this work and our previous work. There are three NP coupling parameters in our previous paper [32]. But only one coupling parameter are shown in this paper. Meanwhile the NP coupling parameter is counteracted in final result $\mathcal{A}_{FB}(B \rightarrow K^{(*)}\ell_i^-\ell_j^+)(s)$.

$$\mathcal{A}_{FB}(B \rightarrow K\ell_i^-\ell_j^+)(s) = -\frac{1}{D_K}|H_t(q^2)H_0(q^2)|\left(\left|h_{\frac{1}{2},\frac{1}{2}}\right|^2 + \left|h_{-\frac{1}{2},-\frac{1}{2}}\right|^2\right), \quad (8)$$

where

$$\begin{aligned} D_K &= \frac{1}{3}|H_0(q^2)|^2\left(\left|h_{\frac{1}{2},\frac{1}{2}}\right|^2 + \left|h_{-\frac{1}{2},-\frac{1}{2}}\right|^2 + \left|h_{\frac{1}{2},-\frac{1}{2}}\right|^2 + \left|h_{-\frac{1}{2},\frac{1}{2}}\right|^2\right) \\ &\quad + |H_t(q^2)|^2\left(\left|h_{\frac{1}{2},\frac{1}{2}}\right|^2 + \left|h_{-\frac{1}{2},-\frac{1}{2}}\right|^2\right). \end{aligned} \quad (9)$$

and for $B \rightarrow K^*\ell_i^-\ell_j^+$, \mathcal{A}_{FB} is same with Eq. (11) from Ref. [32] except

$$\begin{aligned} N_{K^*} &= -2|H_{0t}H_{00}|\left(\left|h_{\frac{1}{2},\frac{1}{2}}\right|^2 + \left|h_{-\frac{1}{2},-\frac{1}{2}}\right|^2\right) + \frac{1}{2}\left(|H_{++}|^2 - |H_{--}|^2\right)\left(\left|h_{\frac{1}{2},-\frac{1}{2}}\right|^2 - \left|h_{-\frac{1}{2},\frac{1}{2}}\right|^2\right), \\ D_{K^*} &= \frac{2}{3}\left(|H_{00}|^2 + |H_{++}|^2 + |H_{--}|^2\right)\left(\left|h_{\frac{1}{2},\frac{1}{2}}\right|^2 + \left|h_{-\frac{1}{2},-\frac{1}{2}}\right|^2 + \left|h_{\frac{1}{2},-\frac{1}{2}}\right|^2 + \left|h_{-\frac{1}{2},\frac{1}{2}}\right|^2\right) \\ &\quad + 2|H_{0t}|^2\left(\left|h_{\frac{1}{2},\frac{1}{2}}\right|^2 + \left|h_{-\frac{1}{2},-\frac{1}{2}}\right|^2\right). \end{aligned} \quad (10)$$

Besides, in this paper we also study the single lepton polarization asymmetries. For the sake of simplicity only the longitudinal component product of single lepton polarization asymmetries $P_i^{\ell^\pm}$ ($i = L$) are studied. The single lepton longitudinal polarization asymmetries are got from [32, 34].

The specific expressions of $\mathcal{P}_L^{\ell^\pm}(B \rightarrow K^{(*)}\ell_i^-\ell_j^+)(s)$ in the scalar leptoquark model are also same with Eq. (14) and (17) our previous paper except $N_K^{\ell^-}, N_K^{\ell^+}, N_{K^*}^{\ell^-}, N_{K^*}^{\ell^+}$ [32].

$$\begin{aligned} N_K^{\ell^-} &= \left\{ \frac{1}{3}|H_0(q^2)|^2\left[\left(\left|h_{\frac{1}{2},\frac{1}{2}}\right|^2 - \left|h_{-\frac{1}{2},-\frac{1}{2}}\right|^2\right) + \left(\left|h_{\frac{1}{2},-\frac{1}{2}}\right|^2 - \left|h_{-\frac{1}{2},\frac{1}{2}}\right|^2\right)\right] \right. \\ &\quad \left. + |H_t(q^2)|^2\left(\left|h_{\frac{1}{2},\frac{1}{2}}\right|^2 - \left|h_{-\frac{1}{2},-\frac{1}{2}}\right|^2\right) \right\}, \end{aligned} \quad (11)$$

$$\begin{aligned} N_K^{\ell^+} &= \left\{ \frac{1}{3}|H_0(q^2)|^2\left[\left(\left|h_{\frac{1}{2},\frac{1}{2}}\right|^2 - \left|h_{-\frac{1}{2},-\frac{1}{2}}\right|^2\right) - \left(\left|h_{\frac{1}{2},-\frac{1}{2}}\right|^2 - \left|h_{-\frac{1}{2},\frac{1}{2}}\right|^2\right)\right] \right. \\ &\quad \left. + |H_t(q^2)|^2\left(\left|h_{\frac{1}{2},\frac{1}{2}}\right|^2 - \left|h_{-\frac{1}{2},-\frac{1}{2}}\right|^2\right) \right\}. \end{aligned} \quad (12)$$

$$\begin{aligned} N_{K^*}^{\ell^-} &= \left\{ \frac{2}{3}\left(|H_{00}|^2 + |H_{++}|^2 + |H_{--}|^2\right)\left[\left(\left|h_{\frac{1}{2},\frac{1}{2}}\right|^2 - \left|h_{-\frac{1}{2},-\frac{1}{2}}\right|^2\right) + \left(\left|h_{\frac{1}{2},-\frac{1}{2}}\right|^2 - \left|h_{-\frac{1}{2},\frac{1}{2}}\right|^2\right)\right] \right. \\ &\quad \left. + 2|H_{0t}|^2\left(\left|h_{\frac{1}{2},\frac{1}{2}}\right|^2 - \left|h_{-\frac{1}{2},-\frac{1}{2}}\right|^2\right) \right\}, \end{aligned} \quad (13)$$

$$\begin{aligned} N_{K^*}^{\ell^+} &= \left\{ \frac{2}{3}\left(|H_{00}|^2 + |H_{++}|^2 + |H_{--}|^2\right)\left[\left(\left|h_{\frac{1}{2},\frac{1}{2}}\right|^2 - \left|h_{-\frac{1}{2},-\frac{1}{2}}\right|^2\right) - \left(\left|h_{\frac{1}{2},-\frac{1}{2}}\right|^2 - \left|h_{-\frac{1}{2},\frac{1}{2}}\right|^2\right)\right] \right. \\ &\quad \left. + 2|H_{0t}|^2\left(\left|h_{\frac{1}{2},\frac{1}{2}}\right|^2 - \left|h_{-\frac{1}{2},-\frac{1}{2}}\right|^2\right) \right\}. \end{aligned} \quad (14)$$

By comparing, we find that the difference between this work and our previous work is the hadronic and leptonic helicity amplitudes shown in above Eqs. (8) – (14).

3 Numerical results and analysis

In this section we investigate the scalar LQ effects on the aforementioned physical observed quantity of the process $B_s \rightarrow \ell_i^- \ell_j^+$ and $B \rightarrow K^{(*)} \ell_i^- \ell_j^+$. In this work instead of using the experimental branching ratios of the $B_s \rightarrow \mu^- \mu^+$ [35–37], the latest experimental measurements of $B_s \rightarrow \ell_i^- \ell_j^+$ and $B \rightarrow K^{(*)} \ell_i^- \ell_j^+$ are used to constraint the leptoquark parameters and this method is more convenient and intuitively clear. From Eqs. (2) and (4) in Sect. 2 we know that there are two types effective hamiltonian in leptoquark model and this leads to a slight different results when calculate the hadronic and leptonic helicity amplitudes for two molds in Appendix. As discussed in the Appendix the axial-vector current matrix elements $\langle K(p_K) | \bar{s} \gamma^\mu \gamma_5 b | B(p_B) \rangle = 0$ lead to the hadronic helicity amplitudes are same with each other in mold A and mold B for process $B \rightarrow K \ell_i^- \ell_j^+$. Unlike the process $B \rightarrow K \ell_i^- \ell_j^+$, the hadronic helicity amplitudes of $B \rightarrow K^* \ell_i^- \ell_j^+$ are different from each other in this two molds since $\langle K^*(p_{K^*}) | \bar{s} \gamma^\mu \gamma_5 b | B(p_B) \rangle \neq 0$. However, we find these differences in Eqs. (2) and (4) has little effect on the final result because hadronic (leptonic) helicity amplitudes displayed in Eqs. (18) and (21) in this two molds are equal or opposite.

The bounds on leptoquark coupling of $B_q \rightarrow \mu^+ \mu^-$ are also displayed in many articles. However, these articles do not give the clear bounds of leptoquark coupling for the LFV process $B \rightarrow K^{(*)} \ell_i^- \ell_j^+$ [23–26]. It is noteworthy that this article presents detailed calculation for leptoquark couplings and show the effect of scalar leptoquark on many physical quantities with tables and graphics for the processes $B \rightarrow K^{(*)} \ell_i^- \ell_j^+$. First, the use of recent experimental measurements of the LFV decays $\mathcal{B}(B_s \rightarrow \ell_i^- \ell_j^+)$ and $\mathcal{B}(B \rightarrow K^{(*)} \ell_i^- \ell_j^+)$, leads to constraint the upper limits on the relevant NP coupling parameter space. Then we investigate the constrained NP coupling effects on the branching ratios, the dileptonic invariant mass spectra, forward-backward asymmetries and the single lepton longitudinal polarization asymmetries of B meson decay processes. The relevant input parameters, experimental upper limits at 90% C.L and form factors used in this paper are mainly from Refs. [38–40].

Now, using the experimental upper limits displayed in the second columns of Tabs. 1-2, we constrain the allowed spaces of the relevant NP coupling products. Our numerical LFV predictions of the branching ratios due to scalar leptoquark exchange are listed in the last two columns of Tabs.

1-2. From this two tables we find the following remarks. (I) the result of these processes in this two molds are almost the same everywhere. This corroborates that the difference in Hamiltonian has little influence on the final result. This phenomenon is consistent with many literatures which only analyze the effect of a mold scalar leptoquark [23–26]. (II) For $\bar{b} \rightarrow \bar{s}e^-\mu^+, \bar{s}\mu^-e^+$ transitions, the experimental upper limits of all relevant branching ratios are reported and the limits of the NP coupling products mainly come from the processes $B_u^+ \rightarrow K^+\ell_i^-\ell_j^+$. The upper limits of the restrained NP coupling parameter space are shown in the third column of Tab. 3. From Tab. 3 we find that the moduli of the restrained NP coupling products appeared in this six processes are strongly restricted by present measurements. At the same time we also find that the moduli of the LNV coupling products appeared in $\bar{b} \rightarrow \bar{s}e^-\mu^+, \bar{s}\mu^-e^+$ transitions are stronger. The last column listed in Tab. 3 are previous upper limits. The indices “a” and “b” denote the processes that give the constrained of the coupling products in Ref. [23–26, 41, 42]. All the couplings λ and λ^* in Ref. [42] are real and equal to each

Table 1: The experimental upper limits at 90% C.L. [38] and Leptoquark predictions for $\bar{b} \rightarrow \bar{s}e^-\mu^+, \bar{s}\mu^-e^+, \bar{s}e^-\tau^+$ respectively.

	Exp. Limits	mold A X=(3,2,7/6)	mold B X=(3,2,1/6)
$\mathcal{B}(B_s \rightarrow e^-\mu^+)(\times 10^{-8})$	≤ 1.1	≤ 0.04	≤ 0.04
$\mathcal{B}(B_d^0 \rightarrow K^0e^-\mu^+)(\times 10^{-7})$	≤ 2.7	≤ 1.20	≤ 1.20
$\mathcal{B}(B_u^+ \rightarrow K^+e^-\mu^+)(\times 10^{-7})$	≤ 1.3	≤ 1.29	≤ 1.29
$\mathcal{B}(B_d^0 \rightarrow K^{*0}e^-\mu^+)(\times 10^{-7})$	≤ 3.4	≤ 3.39	≤ 3.40
$\mathcal{B}(B_u^+ \rightarrow K^{*+}e^-\mu^+)(\times 10^{-7})$	≤ 9.9	≤ 3.69	≤ 3.69
$\mathcal{B}(B_s \rightarrow \mu^-e^+)(\times 10^{-8})$	≤ 1.1	≤ 0.03	≤ 0.03
$\mathcal{B}(B_d^0 \rightarrow K^0\mu^-e^+)(\times 10^{-7})$	≤ 2.7	≤ 0.85	≤ 0.85
$\mathcal{B}(B_u^+ \rightarrow K^+\mu^-e^+)(\times 10^{-8})$	≤ 9.1	≤ 9.09	≤ 9.09
$\mathcal{B}(B_d^0 \rightarrow K^{*0}\mu^-e^+)(\times 10^{-7})$	≤ 5.3	≤ 3.51	≤ 3.79
$\mathcal{B}(B_u^+ \rightarrow K^{*+}\mu^-e^+)(\times 10^{-6})$	≤ 1.3	≤ 0.38	≤ 0.41
$\mathcal{B}(B_s \rightarrow e^-\tau^+)(\times 10^{-5})$...	≤ 1.65	≤ 1.65
$\mathcal{B}(B_d^0 \rightarrow K^0e^-\tau^+)(\times 10^{-5})$...	≤ 1.39	≤ 1.39
$\mathcal{B}(B_u^+ \rightarrow K^+e^-\tau^+)(\times 10^{-5})$	≤ 1.5	≤ 1.49	≤ 1.49
$\mathcal{B}(B_d^0 \rightarrow K^{*0}e^-\tau^+)(\times 10^{-5})$...	≤ 4.11	≤ 4.19
$\mathcal{B}(B_u^+ \rightarrow K^{*+}e^-\tau^+)(\times 10^{-5})$...	≤ 4.46	≤ 4.57

Table 2: The experimental upper limits at 90% C.L. [38] and Leptoquark predictions for $\bar{b} \rightarrow \bar{s}\tau^-e^+, \bar{s}\mu^-\tau^+, \bar{s}\tau^-\mu^+$ respectively.

	Exp. Limits	mold A X=(3,2,7/6)	mold B X=(3,2,1/6)
$\mathcal{B}(B_s \rightarrow \tau^-e^+)(\times 10^{-5})$...	≤ 5.23	≤ 5.23
$\mathcal{B}(B_d^0 \rightarrow K^0\tau^-e^+)(\times 10^{-5})$...	≤ 3.99	≤ 3.99
$\mathcal{B}(B_u^+ \rightarrow K^+\tau^-e^+)(\times 10^{-5})$	≤ 4.3	≤ 4.29	≤ 4.29
$\mathcal{B}(B_d^0 \rightarrow K^{*0}\tau^-e^+)(\times 10^{-5})$...	≤ 12.99	≤ 12.94
$\mathcal{B}(B_u^+ \rightarrow K^{*+}\tau^-e^+)(\times 10^{-5})$...	≤ 12.04	≤ 12.09
$\mathcal{B}(B_s \rightarrow \mu^-\tau^+)(\times 10^{-5})$...	≤ 3.25	≤ 3.25
$\mathcal{B}(B_d^0 \rightarrow K^0\mu^-\tau^+)(\times 10^{-5})$...	≤ 2.60	≤ 2.60
$\mathcal{B}(B_u^+ \rightarrow K^+\mu^-\tau^+)(\times 10^{-5})$	≤ 2.8	≤ 2.80	≤ 2.80
$\mathcal{B}(B_d^0 \rightarrow K^{*0}\mu^-\tau^+)(\times 10^{-5})$...	≤ 7.64	≤ 8.21
$\mathcal{B}(B_u^+ \rightarrow K^{*+}\mu^-\tau^+)(\times 10^{-5})$...	≤ 8.29	≤ 8.31
$\mathcal{B}(B_s \rightarrow \tau^-\mu^+)(\times 10^{-5})$...	≤ 5.47	≤ 5.47
$\mathcal{B}(B_d^0 \rightarrow K^0\tau^-\mu^+)(\times 10^{-5})$...	≤ 4.18	≤ 4.18
$\mathcal{B}(B_u^+ \rightarrow K^+\tau^-\mu^+)(\times 10^{-5})$	≤ 4.5	≤ 4.50	≤ 4.50
$\mathcal{B}(B_d^0 \rightarrow K^{*0}\tau^-\mu^+)(\times 10^{-5})$...	≤ 12.45	≤ 12.50
$\mathcal{B}(B_u^+ \rightarrow K^{*+}\tau^-\mu^+)(\times 10^{-5})$...	≤ 14.60	≤ 14.58

other and the leptoquark mass M_s are 500GeV[42] and 100GeV[41], which method is indicated “a”. The bounds for the relevant coupling $B \rightarrow \ell^+\ell^-$ are listed in Tab. I in Ref. [26, 27] and Tab. II in Ref. [24], which method is indicated “b”. It is worthwhile to note that the limits of the processes $\bar{b} \rightarrow \bar{s}\mu^-e^+, \bar{b} \rightarrow \bar{s}\tau^-e^+$ and $\bar{b} \rightarrow \bar{s}\tau^-\mu^+$ are not listed in Tab. 3. Because in that papers only process $\bar{b} \rightarrow \bar{s}\ell_i^-\ell_j^+(j > i)$ are studied [24, 26, 27]. It is clear to find that our upper limits are stronger than previous ones “a” which mainly come from process $B \rightarrow X\ell\nu(\ell\ell)$ besides $K \rightarrow \pi\nu\nu$.

Using the upper limits of the constrained coupling parameter spaces listed in Tab. 3, we next investigate the NP effects on the branching ratios, the dilepton invariant mass spectra, the differential forward-backward asymmetries and the single lepton longitudinal polarization asymmetries of the B meson decay.

Noted that, after detailed researching, we find that the difference of the effect for two molds is not significant except the single lepton longitudinal polarization asymmetries ($P_L^{\ell^\pm}$) in the final result of

Table 3: Limits for the relevant NP coupling parameters by $B_s \rightarrow \ell_i^- \ell_j^+$ and $B \rightarrow K^{(*)} \ell_i^- \ell_j^+$ decays and previous bounds are listed for comparison (in units of GeV^{-2}). The index “a” illustrate that bounds mainly come from Ref.[41, 42] and “b” come from Refs.[24, 26, 27].

LFV couplings	Relevant processes	Our bounds	Previous bounds
Mold A $\frac{ \lambda^{13}\lambda^{22*} }{M_s^2}$	$\bar{b} \rightarrow \bar{s} e^- \mu^+$	$\leq 6.60 \times 10^{-9}$	$3 \times 10^{-7} [B \rightarrow K \bar{e} \mu]_a$
Mold B $\frac{ \lambda^{21}\lambda^{32*} }{M_s^2}$		$\leq 6.61 \times 10^{-9}$	$1.32 \times 10^{-9}_b$ $2 \times 10^{-9} [K \rightarrow \pi \nu \bar{\nu}]_a$
Mold A $\frac{ \lambda^{23}\lambda^{12*} }{M_s^2}$	$\bar{b} \rightarrow \bar{s} \mu^- e^+$	$\leq 5.57 \times 10^{-9}$	$3 \times 10^{-7} [B \rightarrow K \bar{e} \mu]_a$
Mold B $\frac{ \lambda^{22}\lambda^{31*} }{M_s^2}$		$\leq 5.57 \times 10^{-9}$	$2 \times 10^{-9} [K \rightarrow \pi \nu \bar{\nu}]_a$
Mold A $\frac{ \lambda^{13}\lambda^{32*} }{M_s^2}$	$\bar{b} \rightarrow \bar{s} e^- \tau^+$	$\leq 9.15 \times 10^{-8}$	$4 \times 10^{-6} [B \rightarrow X \ell \nu]_a$
Mold B $\frac{ \lambda^{21}\lambda^{33*} }{M_s^2}$		$\leq 9.17 \times 10^{-8}$	$6.51 \times 10^{-9}_b$ $2 \times 10^{-7} [B \rightarrow X \tau \bar{\mu}]_a$
Mold A $\frac{ \lambda^{33}\lambda^{12*} }{M_s^2}$	$\bar{b} \rightarrow \bar{s} \tau^- e^+$	$\leq 1.59 \times 10^{-7}$	$4 \times 10^{-6} [B \rightarrow X \ell \nu]_a$
Mold B $\frac{ \lambda^{23}\lambda^{31*} }{M_s^2}$		$\leq 1.58 \times 10^{-7}$	$2 \times 10^{-7} [B \rightarrow X \tau \bar{\mu}]_a$
Mold A $\frac{ \lambda^{23}\lambda^{32*} }{M_s^2}$	$\bar{b} \rightarrow \bar{s} \mu^- \tau^+$	$\leq 1.28 \times 10^{-7}$	$2 \times 10^{-7} [B \rightarrow X \tau \bar{\mu}]_a$
Mold B $\frac{ \lambda^{22}\lambda^{33*} }{M_s^2}$		$\leq 1.28 \times 10^{-7}$	$1.25 \times 10^{-5}_b$ $2 \times 10^{-7} [B \rightarrow X \tau \bar{\mu}]_a$
Mold A $\frac{ \lambda^{33}\lambda^{22*} }{M_s^2}$	$\bar{b} \rightarrow \bar{s} \tau^- \mu^+$	$\leq 1.63 \times 10^{-7}$	$2 \times 10^{-7} [B \rightarrow X \tau \bar{\mu}]_a$
Mold B $\frac{ \lambda^{23}\lambda^{32*} }{M_s^2}$		$\leq 1.61 \times 10^{-7}$	$2 \times 10^{-7} [B \rightarrow X \tau \bar{\mu}]_a$

two molds. We find that all branching ratios are very sensitive to and great increasing with the moduli of NP couplings parameters and this is similar with the effects due to the squark exchange coupling $\lambda'_{jk3} \lambda'^*_{ik2}$ in our previous papers except the specific data is different [32]. So we do not display the NP coupling effect on branching ratios of the LFV process $\bar{b} \rightarrow \bar{s} \ell_i^- \ell_j^+$.

Besides, the contributions on $d\mathcal{B}/ds$ and A_{FB} for $B^+ \rightarrow K^{(*)+} \ell_i^- \ell_j^+$ due to the scalar leptoquark exchange in this two molds are also investigated. Fortunately, the variation trend of this two physical quantities are also similar with the article [32]. For simplicity, this article doesn't show the effect on $d\mathcal{B}/ds$ and A_{FB} anymore. Nevertheless, it is worthwhile to note that the variation trends of $d\mathcal{B}/ds$ for $B^+ \rightarrow K^+ \ell_i^- \ell_j^+$ is consistent with Ref [26, 27]. However, the variation trends of $d\mathcal{B}/ds$ for process $B^+ \rightarrow K^{*+} \ell_i^- \ell_j^+$ are different from the [26]. The cause of this difference is mainly from that the author

have neglected the mass of the kaon, pion, muon and electron for simplicity. In this paper we consider the mass of all particles in our calculation.

It is regrettable that no literature has investigated the A_{FB} and $P_L^{\ell^\pm}$ for relevant LFV semileptonic $B \rightarrow K^{(*)} \ell_i^- \ell_j^+$ decays in the scalar leptoquark model so far [23–26]. In our previous paper we clearly display the RPV coupling effect on A_{FB} and $P_L^{\ell^\pm}$ in the form of a two-dimensional scatter plots for three NP couplings [32]. After accurate calculation and inquiry, we find that the NP coupling effect on A_{FB} due to scalar leptoquark exchange is similar with our article [32].

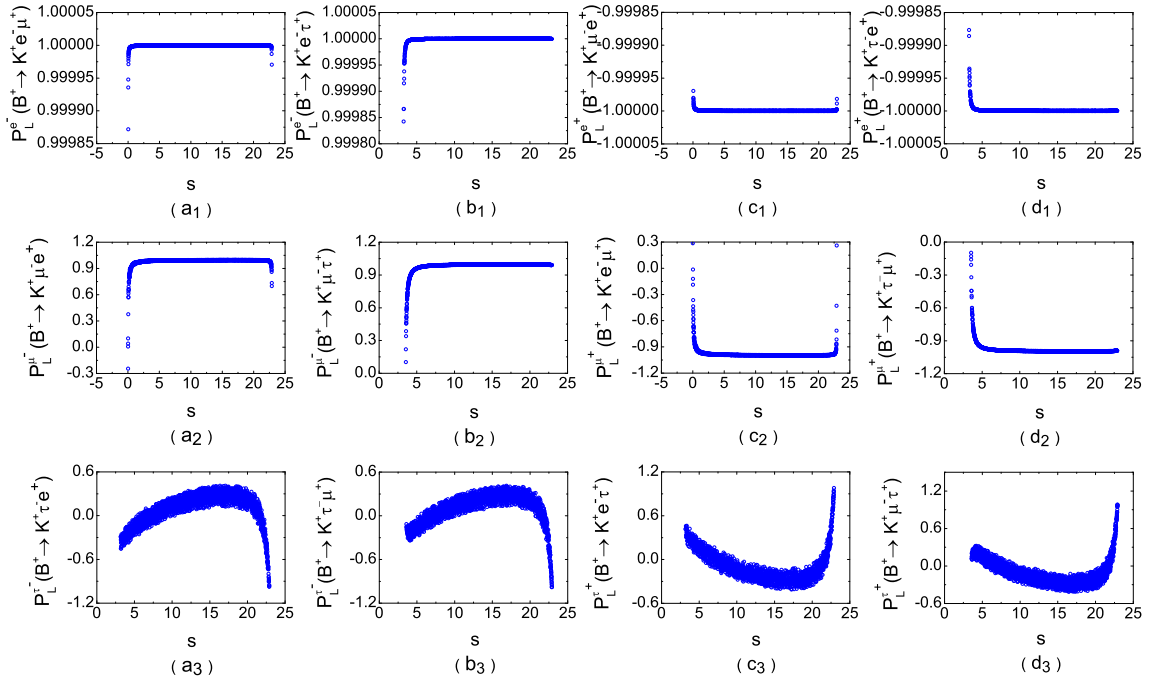


Figure 2: The effects on $P_L^{\ell^\pm}$ in $B^+ \rightarrow K^+ \ell_i^- \ell_j^+$ decays in mold A $X=(3,2,7/6)$.

Last but not least, for $P_L^{\ell^\pm}$, the effect due to scalar leptoquark exchange has slight difference between mold A and mold B. So we mainly investigate the effect on $(P_L^{\ell^\pm})$ in two molds. From the expression given in Eqs. (11)-(14), we know the $P_L^{\ell^\pm}$ due to the scalar leptoquark exchange depend on the lepton masses, relevant form factors and s besides the NP coupling parameter. We take $B^+ \rightarrow K^{(*)+} \ell_i^- \ell_j^+$ decays as an example, which is shown by Figs. 2–3 and 4–5 in mold A and mold B respectively. The blue, and olive scattered point in Figs. 2–5 represent the process $B^+ \rightarrow K^+ \ell_i^- \ell_j^+$ and $B^+ \rightarrow K^{*+} \ell_i^- \ell_j^+$ respectively. After detailed comparative analysis between this article and the paper [32], we find that the Figs. 4–5 for mold B displayed in this paper are very similar with the effects due to the squark exchange coupling $\lambda'_{jk3} \lambda'_{ik2}$ in our previous paper [32]. All the variation trend of Figs. 4–5 for mold B are extended to Figs. 2-3 and the LNV coupling to the relevant semileptonic B

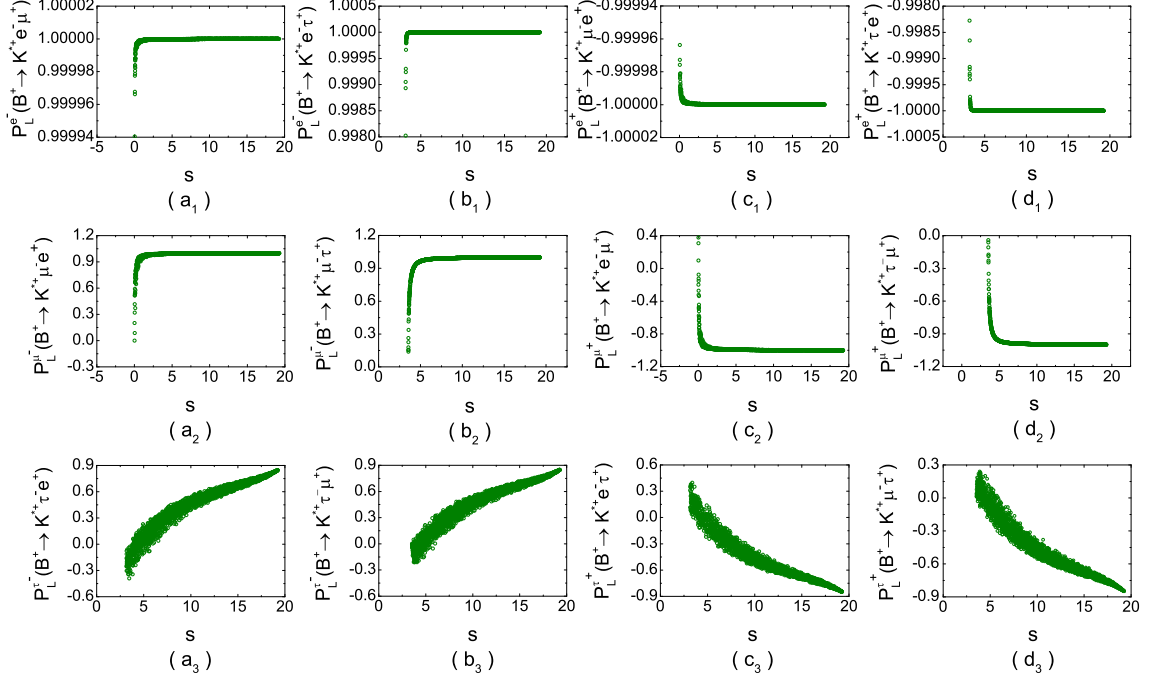


Figure 3: The effects on $P_L^{\ell^\pm}$ in $B^+ \rightarrow K^{*+} \ell_i^- \ell_j^+$ decays in mold A $X=(3,2,7/6)$.

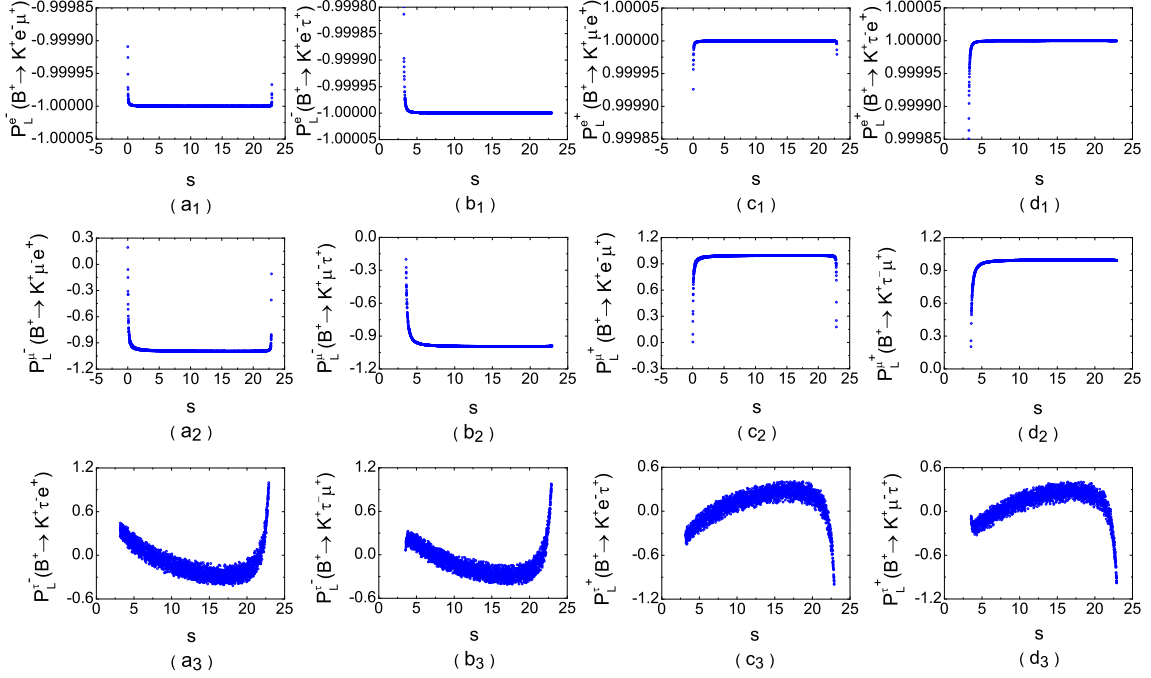


Figure 4: The effects on $P_L^{\ell^\pm}$ in $B^+ \rightarrow K^+ \ell_i^- \ell_j^+$ decays in mold B $X=(3,2,1/6)$.

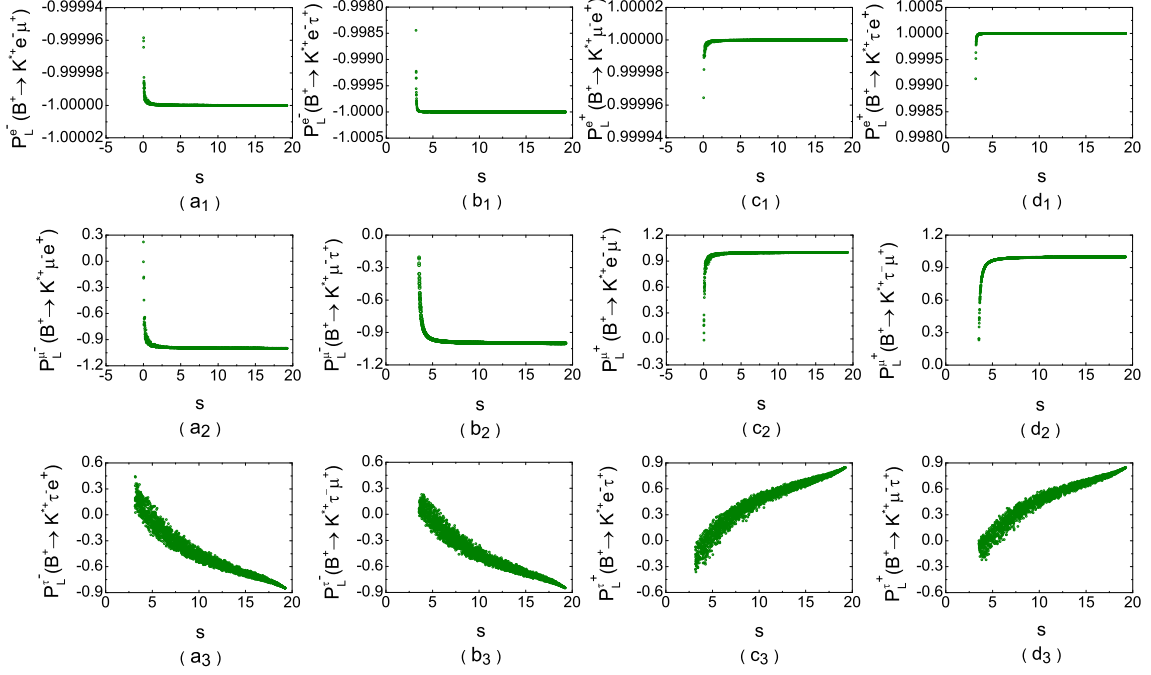


Figure 5: The effects on $P_L^{\ell^\pm}$ in $B^+ \rightarrow K^{*+} \ell_i^- \ell_j^+$ decays in mold B $X=(3,2,1/6)$.

decays due to leptoquark exchange in mold A. It is very clear to find a phenomenon that the opposite result happens in Figs. 2-3. That is to say the NP effect on the single lepton longitudinal polarization asymmetries due to the scalar leptoquark exchange in mold B have exactly the reverse with mold A. From Section Appendix we find that the reason for this phenomenon is mainly come from the lepton section shown in Eq. (18).

4 Summary and conclusions

In this paper, inspired by the recent anomaly measurements of the LFV decays $h \rightarrow \mu\tau, \ell \rightarrow \ell\gamma, Z \rightarrow \ell\ell'$ and the lepton flavor non-universality in decays $\bar{b} \rightarrow \bar{s}\ell^-\ell^+$, we have investigated the NP effects due to the scalar leptoquarks exchange in the processes $B_s \rightarrow \ell_i^-\ell_j^+$ and $B \rightarrow K^{(*)}\ell_i^-\ell_j^+$.

The use of latest experimental measurements of $\mathcal{B}(B_s \rightarrow \ell_i^-\ell_j^+)$ and $\mathcal{B}(B \rightarrow K^{(*)}\ell_i^-\ell_j^+)$ and the theoretical uncertainties at 90% C.L leads to the constrained leptoquark parameter space. We get the very strong bounds on the moduli of the LNV coupling parameters in scalar leptoquark model involving in the $\bar{b} \rightarrow \bar{s}\ell_i^-\ell_j^+$. Moreover, our bounds of these LFV coupling parameters are stronger than the previous ones. The possible NP effects in these LFV B decays have been predicted due

to the scalar leptoquark exchange by using the allowed LNV couplings spaces. It is clear to find that all the branching ratios are very sensitive to and great increasing with the moduli of the LNV coupling products due to scalar leptoquark exchange in mold A and mold B respectively. Moreover, the allowed effects of the scalar leptoquark exchange couplings on other physical observed quantity are also discussed and these observed quantities were not discussed in previous papers about scalar leptoquark model yet. After discussion, it is clear to find following scenarios: the constrained NP coupling have quite obvious effect on the forward-backward asymmetries of these B decay processes. At the same time, particularly for the single lepton longitudinal polarization asymmetries, we find that the NP couplings effects on the LFV semileptonic decays of B meson have opposite result in two molds. In this work the analysis has been performed for the scalar leptoquarks case. In the future, it is possible that the vector leptoquarks may also contribute to the LFV decay process of B meson.

With the rapid development of LHCb and forthcoming Belle-II experiments, the results we get in this work could be a perfect way to probe the NP effects, and will correlate strongly with study for the leptoquark signals in the future experiments.

Acknowledgments

The work was supported by the National Natural Science Foundation of China under contracts 11675137, 11225523, 11775092, 11047145, Nanhu Scholars Program and the High Performance Computing Lab of Xinyang Normal University.

Appendix

Similar with the Appendix of our previous work [32], we can get the following expressions

$$|\mathcal{M}(B \rightarrow K^{(*)} \ell_i^+ \ell_j^-)|^2 = |\mathcal{M}|^2, \quad (15)$$

where

$$|\mathcal{M}|^2 = |G_{LQ}|^2 |\langle M | \bar{s} \gamma^\mu (1 + \gamma_5) b | B \rangle \bar{\ell}_i \gamma_\mu (1 - \gamma_5) \ell_j |^2 \equiv |G_{LQ}|^2 |L_{\mu\nu} H^{\mu\nu}|, \quad (16)$$

with G_{LQ} is G_{LQ}^1 (G_{LQ}^7) which is from Eq. (2) and Eq. (4).

A Formulae of the $B \rightarrow K \ell_i^- \ell_j^+$ decays

Because the axial-vector current matrix elements $\langle K(p_K) | \bar{s} \gamma^\mu \gamma_5 b | B(p_B) \rangle = 0$, we find that the hadronic helicity amplitudes are same with each other for $X = (3, 2, 7/6)$ and $X = (3, 2, 1/6)$.

The the helicity amplitudes for $B \rightarrow K \ell_i^- \ell_j^+$ we use in this paper for scalar leptoquark model are same with the $H_0(q^2)$ and $H_t(q^2)$ shown in Eq. (26) of our paper [32]. For the form factor for $H_0(q^2)$ and $H_t(q^2)$ are from Refs. [39, 40]

Similar to the method in Refs. [43, 44] we obtain the form of lepton helicity amplitudes in the leptoquark model.

$$\begin{aligned} h_{\lambda_{\ell_i}=\mp\frac{1}{2}, \lambda_{\ell_j}=\mp\frac{1}{2}}^7 &= \bar{u}_{\ell_i}(\pm\frac{1}{2})\gamma^\mu(1+\gamma_5)v_{\ell_j}(\pm\frac{1}{2}) \begin{Bmatrix} \epsilon_\mu(\pm 1) \\ \epsilon_\mu(t), \epsilon_\mu(0) \end{Bmatrix}, \\ h_{\lambda_{\ell_i}=\mp\frac{1}{2}, \lambda_{\ell_j}=\mp\frac{1}{2}}^1 &= \bar{u}_{\ell_i}(\pm\frac{1}{2})\gamma^\mu(1-\gamma_5)v_{\ell_j}(\pm\frac{1}{2}) \begin{Bmatrix} \epsilon_\mu(\pm 1) \\ \epsilon_\mu(t), \epsilon_\mu(0) \end{Bmatrix}, \end{aligned} \quad (17)$$

the superscript of h represent $X = (3, 2, 1/6)$ and $X = (3, 2, 7/6)$ respectively. For mold B $X = (3, 2, 1/6)$ the lepton helicity amplitudes are same with h^1 listed in Eq. (28) due to squark exchange in RPV SUSY model [32]. For mold A $X = (3, 2, 7/6)$ the lepton helicity amplitudes

$$\begin{aligned} \left| h_{\frac{1}{2}, \frac{1}{2}}^7 \right|^2 &= \frac{1}{s} \left[s^2 - (m_{\ell_j}^2 - m_{\ell_i}^2 - \sqrt{\lambda_L})^2 \right], \\ \left| h_{\frac{1}{2}, -\frac{1}{2}}^7 \right|^2 &= 4 \left(s - m_{\ell_i}^2 - m_{\ell_j}^2 + \sqrt{\lambda_L} \right), \\ \left| h_{-\frac{1}{2}, \frac{1}{2}}^7 \right|^2 &= 4 \left(s - m_{\ell_i}^2 - m_{\ell_j}^2 - \sqrt{\lambda_L} \right), \\ \left| h_{-\frac{1}{2}, -\frac{1}{2}}^7 \right|^2 &= \frac{1}{s} \left[s^2 - (m_{\ell_i}^2 - m_{\ell_j}^2 - \sqrt{\lambda_L})^2 \right], \end{aligned} \quad (18)$$

with $\lambda_L \equiv \lambda(m_{\ell_i}^2, m_{\ell_j}^2, s)$. It is easy to find a phenomena that the results between mold A and mold B are equal.

For processes $B \rightarrow K \ell_i^- \ell_j^+$, the double differential decay rates with λ_ℓ can be represented as

$$\begin{aligned} \frac{d^2\Gamma^K[\lambda_{\ell_i}=\frac{1}{2}, \lambda_{\ell_j}=\frac{1}{2}]}{dsd\cos\theta} &= \frac{u(s)|G_{LQ}|^2}{29\pi^3 m_B^3 s} \left\{ \left| h_{\frac{1}{2}, \frac{1}{2}} \right|^2 |H_t(q^2) - H_0(q^2) \cos\theta|^2 \right\}, \\ \frac{d^2\Gamma^K[\lambda_{\ell_i}=-\frac{1}{2}, \lambda_{\ell_j}=\frac{1}{2}]}{dsd\cos\theta} &= \frac{u(s)|G_{LQ}|^2}{29\pi^3 m_B^3 s} \left\{ \frac{1}{2} \left| h_{-\frac{1}{2}, \frac{1}{2}} \right|^2 |H_0(q^2)|^2 \sin^2\theta \right\}, \\ \frac{d^2\Gamma^K[\lambda_{\ell_i}=\frac{1}{2}, \lambda_{\ell_j}=-\frac{1}{2}]}{dsd\cos\theta} &= \frac{u(s)|G_{LQ}|^2}{29\pi^3 m_B^3 s} \left\{ \frac{1}{2} \left| h_{\frac{1}{2}, -\frac{1}{2}} \right|^2 |H_0(q^2)|^2 \sin^2\theta \right\}, \\ \frac{d^2\Gamma^K[\lambda_{\ell_i}=-\frac{1}{2}, \lambda_{\ell_j}=-\frac{1}{2}]}{dsd\cos\theta} &= \frac{u(s)|G_{LQ}|^2}{29\pi^3 m_B^3 s} \left\{ \left| h_{-\frac{1}{2}, -\frac{1}{2}} \right|^2 |H_t(q^2) - H_0(q^2) \cos\theta|^2 \right\}, \end{aligned} \quad (19)$$

with

$$G_{LQ} = \begin{cases} G_{LQ}^{\frac{1}{6}} & \text{for } X = (3, 2, 1/6) \\ G_{LQ}^{\frac{7}{6}} & \text{for } X = (3, 2, 7/6) \end{cases} \quad (20)$$

B Formulae of the $B \rightarrow K^* \ell_i^- \ell_j^+$ decays

Unlike the process $B \rightarrow K$, the hadronic helicity amplitudes of $B \rightarrow K^*$ are different from each other between $X = (3, 2, 1/6)$ and $X = (3, 2, 7/6)$ because the $B \rightarrow K^*$ matrix element for the axial-vector current don't vanishes.

For mold B $X = (3, 2, 1/6)$, the hadronic helicity amplitudes are same with $H^1(q^2)$ listed in Eq. (34) due to squark exchange in RPV SUSY model [32]. And for mold A $X = (3, 2, 7/6)$ Then we can obtain the helicity amplitudes written as

$$\begin{aligned} H_{\pm\pm}^7(q^2) &= -(m_B + m_{K^*})A_1(q^2) \mp \frac{2m_B}{m_B + m_{K^*}}|\vec{\mathbf{p}}|V(q^2), \\ H_{00}^7(q^2) &= -\frac{1}{2m_{K^*}\sqrt{q^2}} \left[(m_B^2 - m_{K^*}^2 - q^2)(m_B + m_{K^*})A_1(q^2) - \frac{4m_B^2|\vec{\mathbf{p}}|^2}{m_B + m_{K^*}}A_2(q^2) \right], \\ H_{0t}^7(q^2) &= -\frac{2m_B|\vec{\mathbf{p}}|}{\sqrt{q^2}}A_0(q^2), \end{aligned} \quad (21)$$

with $|\vec{\mathbf{p}}| = \frac{\sqrt{\lambda(m_B^2, m_{K^*}^2, s)}}{2m_B}$. At the same time it is clear to find hadronic helicity amplitudes in this two molds are opposite.

We can also get the double differential decay rates for $B \rightarrow K^* \ell_i^- \ell_j^+$

$$\begin{aligned} \frac{d^2\Gamma^{K^*}[\lambda_{\ell_i} = \frac{1}{2}, \lambda_{\ell_j} = \frac{1}{2}]}{dsd\cos\theta} &= \frac{u(s)|G_{LQ}|^2}{2^9\pi^3m_B^3s} \left\{ \left| h_{\frac{1}{2}, \frac{1}{2}} \right|^2 \left[|H_{0t} - H_{00}\cos\theta|^2 \right. \right. \\ &\quad \left. \left. + \frac{1}{2}|H_{++}|^2\sin^2\theta + \frac{1}{2}|H_{--}|^2\sin^2\theta \right] \right\}, \\ \frac{d^2\Gamma^{K^*}[\lambda_{\ell_i} = -\frac{1}{2}, \lambda_{\ell_j} = \frac{1}{2}]}{dsd\cos\theta} &= \frac{u(s)|G_{LQ}|^2}{2^9\pi^3m_B^3s} \left\{ \left| h_{-\frac{1}{2}, \frac{1}{2}} \right|^2 \left[\frac{1}{2}|H_{00}|^2\sin^2\theta \right. \right. \\ &\quad \left. \left. + \frac{1}{4}|H_{++}|^2(1 - \cos\theta)^2 + \frac{1}{4}|H_{--}|^2(1 + \cos\theta)^2 \right] \right\}, \\ \frac{d^2\Gamma^{K^*}[\lambda_{\ell_i} = \frac{1}{2}, \lambda_{\ell_j} = -\frac{1}{2}]}{dsd\cos\theta} &= \frac{u(s)|G_{LQ}|^2}{2^9\pi^3m_B^3s} \left\{ \left| h_{\frac{1}{2}, -\frac{1}{2}} \right|^2 \left[\frac{1}{2}|H_{00}|^2\sin^2\theta \right. \right. \\ &\quad \left. \left. + \frac{1}{4}|H_{++}|^2(1 + \cos\theta)^2 + \frac{1}{4}|H_{--}|^2(1 - \cos\theta)^2 \right] \right\}, \\ \frac{d^2\Gamma^{K^*}[\lambda_{\ell_i} = -\frac{1}{2}, \lambda_{\ell_j} = -\frac{1}{2}]}{dsd\cos\theta} &= \frac{u(s)|G_{LQ}|^2}{2^9\pi^3m_B^3s} \left\{ \left| h_{-\frac{1}{2}, -\frac{1}{2}} \right|^2 \left[|H_{0t} - H_{00}\cos\theta|^2 \right. \right. \\ &\quad \left. \left. + \frac{1}{2}|H_{++}|^2\sin^2\theta + \frac{1}{2}|H_{--}|^2\sin^2\theta \right] \right\}, \end{aligned} \quad (22)$$

References

- [1] R. Aaij *et al.* [LHCb Collaboration], JHEP **1708**, 055 (2017) [arXiv:1705.05802 [hep-ex]].

- [2] S. Descotes-Genon, J. Matias and J. Virto, Phys. Rev. D **88**, 074002 (2013) [arXiv:1307.5683 [hep-ph]].
- [3] A. Abdesselam *et al.* [Belle Collaboration], arXiv:1604.04042 [hep-ex].
- [4] S. Wehle *et al.* [Belle Collaboration], Phys. Rev. Lett. **118**, no. 11, 111801 (2017) [arXiv:1612.05014 [hep-ex]].
- [5] F. Happacher *et al.* [Mu2e Collaboration], JINST **12**, no. 09, P09017 (2017).
- [6] A. Nehr Korn [CMS Collaboration], Nucl. Part. Phys. Proc. **287-288**, 160 (2017).
- [7] CMS Collaboration [CMS Collaboration], CMS-PAS-HIG-17-001.
- [8] S. L. Glashow, D. Guadagnoli and K. Lane, Phys. Rev. Lett. **114**, 091801 (2015) [arXiv:1411.0565 [hep-ph]].
- [9] D. Be?irevi?, S. Fajfer and N. Ko?nik, Phys. Rev. D **92**, no. 1, 014016 (2015) [arXiv:1503.09024 [hep-ph]].
- [10] H. Georgi and S. L. Glashow, Phys. Rev. Lett. **32**, 438 (1974).
- [11] J. C. Pati and A. Salam, Phys. Rev. D **10**, 275 (1974) Erratum: [Phys. Rev. D **11**, 703 (1975)].
- [12] B. Schrempp and F. Schrempp, Phys. Lett. **153B**, 101 (1985).
- [13] B. Gripaios, JHEP **1002**, 045 (2010) [arXiv:0910.1789 [hep-ph]].
- [14] D. B. Kaplan, Nucl. Phys. **B 365**, 259 (1991).
- [15] I. Dorsner, S. Fajfer, J. F. Kamenik and N. Kosnik, Phys. Lett. B **682**, 67 (2009) [arXiv:0906.5585 [hep-ph]].
- [16] S. Fajfer and N. Kosnik, Phys. Rev. D **79**, 017502 (2009) [arXiv:0810.4858 [hep-ph]].
- [17] A. V. Povarov and A. D. Smirnov, arXiv:1010.5707 [hep-ph].
- [18] J. P. Saha, B. Misra and A. Kundu, Phys. Rev. D **81**, 095011 (2010) [arXiv:1003.1384 [hep-ph]].
- [19] I. Dorsner, J. Drobnak, S. Fajfer, J. F. Kamenik and N. Kosnik, JHEP **1111**, 002 (2011) [arXiv:1107.5393 [hep-ph]].
- [20] N. Kosnik, Phys. Rev. D **86**, 055004 (2012) [arXiv:1206.2970 [hep-ph]].
- [21] F. S. Queiroz, K. Sinha and A. Strumia, Phys. Rev. D **91**, no. 3, 035006 (2015) [arXiv:1409.6301 [hep-ph]].
- [22] B. Allanach, A. Alves, F. S. Queiroz, K. Sinha and A. Strumia, Phys. Rev. D **92**, no. 5, 055023 (2015) [arXiv:1501.03494 [hep-ph]].
- [23] J. M. Arnold, B. Fornal and M. B. Wise, Phys. Rev. D **88**, 035009 (2013) [arXiv:1304.6119 [hep-ph]].

- [24] S. Sahoo and R. Mohanta, Phys. Rev. D **91**, no. 9, 094019 (2015) [arXiv:1501.05193 [hep-ph]].
- [25] R. Mohanta, Phys. Rev. D **89**, no. 1, 014020 (2014) [arXiv:1310.0713 [hep-ph]].
- [26] S. Sahoo and R. Mohanta, Phys. Rev. D **93**, no. 11, 114001 (2016) [arXiv:1512.04657 [hep-ph]].
- [27] R. Mohanta and S. Sahoo, J. Phys. Conf. Ser. **770**, no. 1, 012019 (2016).
- [28] D. Beirevi, N. Konik, O. Sumensari and R. Zukanovich Funchal, JHEP **1611**, 035 (2016) [arXiv:1608.07583 [hep-ph]].
- [29] X. Q. Li, Y. D. Yang and X. Zhang, JHEP **1608**, 054 (2016) [arXiv:1605.09308 [hep-ph]].
- [30] S. W. Wang and Y. D. Yang, Adv. High Energy Phys. **2016**, 5796131 (2016) [arXiv:1608.03662 [hep-ph]].
- [31] X. Q. Li, Y. D. Yang and X. Zhang, JHEP **1702**, 068 (2017) [arXiv:1611.01635 [hep-ph]].
- [32] J. H. Sheng, J. J. Song, R. M. Wang and Y. D. Yang, Nucl. Phys. B **930**, 69 (2018).
- [33] W. Bensalem, D. London, N. Sinha and R. Sinha, Phys. Rev. D **67**, 034007 (2003) [hep-ph/0209228].
- [34] S. R. Choudhury, N. Gaur, A. S. Cornell and G. C. Joshi, Phys. Rev. D **68**, 054016 (2003) [hep-ph/0304084].
- [35] S. Chatrchyan et al., [CMS Collaboration], Phys. Rev. Lett. **111**, 101804 (2013), [arXiv:1307.5025].
- [36] R. Aaij et al., [LHCb Collaboration], Phys. Rev. Lett. **111**, 101805 (2013), [arXiv:1307.5024].
- [37] V. Khachatryan *et al.*, [CMS Collaboration], and I. Bediaga *et al.* [LHCb Collaboration], Nature, **522**, 68 (2015).
- [38] Citation: C.Patrignani et al. (Particle Data Group), Chin. Phys. C 40.100001(2016) and 2017 update.
- [39] P. Ball and R. Zwicky, Phys. Rev. D **71**, 014029 (2005) [hep-ph/0412079].
- [40] Y. L. Wu, M. Zhong and Y. B. Zuo, Rates with Extraction of the CKM parameters " $|V(ub)|, |V(cs)|, |V(cd)|$ " Int. J. Mod. Phys. A **21**, 6125 (2006) [hep-ph/0604007].
- [41] S. Davidson, D. C. Bailey and B. A. Campbell, Z. Phys. C **61**, 613 (1994)[hep-ph/9309310];J. P. Saha, B. Misra and A. Kundu, Phys. Rev. D **81**, 095011 (2010)[arXiv:1003.1384 [hep-ph]].
- [42] R. Benbrik, M. Chabab and G. Faisel, arXiv:1009.3886 [hep-ph].
- [43] J. G. Korner and G. A. Schuler, Z. Phys. C **38** (1988) 511 [Erratum-ibid. C **41** (1989) 690].
- [44] A. Kadeer, J. G. Korner and U. Moosbrugger, Eur. Phys. J. C **59** (2009) 27.